

# Controllable nonlinear effects in an optomechanical resonator containing a quantum well

Eyob A. Sete<sup>1</sup> and H. Eleuch<sup>2</sup><sup>1</sup>*Institute for Quantum Science and Engineering and Department of Physics and Astronomy, Texas A & M University, College Station, Texas 77843, USA*<sup>2</sup>*Max Planck Institute for Physics of Complex Systems, D-01187 Dresden, Germany*

(Received 7 March 2012; published 16 April 2012)

We study nonlinear effects in an optomechanical system containing a quantum well. The nonlinearity due to the optomechanical coupling leads to a bistable behavior in the mean intracavity photon number and substantial squeezing in the transmitted field. We show that the optical bistability and the degree of squeezing can be controlled by tuning the power and frequency of the pump laser. The transmitted field intensity spectrum consists of six distinct peaks corresponding to optomechanical, polariton, and hybrid resonances. Interestingly, even though the quantum well and the mechanical modes are not directly coupled, their interaction with the common quantized cavity mode results in appearance of hybrid resonances.

DOI: [10.1103/PhysRevA.85.043824](https://doi.org/10.1103/PhysRevA.85.043824)

PACS number(s): 42.65.Pc, 42.50.Wk, 42.50.Ct, 42.50.Lc

## I. INTRODUCTION

When one of the mirrors of an optical cavity is set to move, the radiation pressure exerted by the field induces a coupling between its position and the intensity of the cavity field. This modifies the optical path in an intensity-dependent way and leads to nonlinearity in the system. The nonlinearity, which is analogous to Kerr nonlinearity, gives rise to nonclassical features such as quantum noise reduction below the shot-noise level [1] and optical bistability [2–5]. In a pioneering work, Braginsky [6] predicted a classical effect in which the radiation pressure of light field confined in a resonator gives rise to the effect of dynamic back action that is caused by the finite cavity decay time. In recent years, there has been a continuously growing interest in optomechanical systems in connection with the possibility of generating robust continuous-variable entanglement between the mechanical and optical modes [7–10], demonstration of optomechanically induced transparency [11–14], and four wave mixing [5] among others.

From an application viewpoint, optomechanical systems have the potential for ground-state cooling [15–17], optical wavelength conversion of quantum states [18], gravitational wave detection, for example, in the laser interferometer gravitational wave observatory (LIGO) [19,20], and precision force sensing [21]. It is also possible to slow and stop light by using an optomechanical array [22] which will allow the light storage and the realization of compact optical memory. Implementation of these applications requires sufficiently strong optomechanical coupling and high optical and mechanical quality factor. One possible way to enhance the optomechanical coupling is to pump the cavity with a strong laser. Using this method, the strong coupling regime has been observed experimentally [23]. Pumping the cavity with a strong laser also induces nonlinearity in the system which is the source for interesting nonclassical effects.

In this work, we explore the nonlinear and quantum statistical properties of an optomechanical resonator containing a quantum well. In particular, we investigate optical bistability, intensity, and squeezing spectra of the transmitted field. It turns out that the mean intracavity photon number exhibits bistable behavior which can be controlled by the

input pump laser power and frequency. The intensity spectrum of the transmitted field has six distinct peaks corresponding to optomechanical, polariton, and hybrid resonances. The appearance of hybrid peaks—a superposition of polariton and optomechanical resonances—is due to the indirect coupling of the excitons and the mechanical modes via the common cavity mode. We show that such a hybrid resonance can be amplified and/or controlled by tuning the pump power externally for certain parameter regimes. Furthermore, we demonstrate that the transmitted field exhibits a substantial degree of squeezing for optimum pump power at the hybrid resonance frequencies. The generated squeezing can also be controlled by tuning the pump-laser power.

## II. MODEL AND HAMILTONIAN

We consider a generic optomechanical system containing a single quantum well. The schematic of our system is shown in Fig. 1. The mechanical resonator with frequency  $\omega_m$  is subjected to a force proportional to the mean intracavity photon number. The cavity mode of frequency  $\omega_c$  is driven by an intense pump laser of frequency  $\omega_p$  and power  $P$  through the port mirror. In addition, the cavity photons interact with excitons in the quantum well. We assume that the density of excitons is small so that exciton-exciton scattering can be ignored which allows us to treat the exciton-cavity mode interaction linearly. The interaction Hamiltonian of the system is given by

$$H = \hbar\delta_b b^\dagger b + \hbar\Delta a^\dagger a + \frac{1}{2}\hbar\omega_m(p^2 + q^2) + \hbar g(a^\dagger b + b^\dagger a) - \hbar g_m a^\dagger a q + i\hbar\epsilon_p(a^\dagger - a). \quad (1)$$

The first term, with  $\delta_b = \omega_b - \omega_p$  being the pump laser-exciton detuning, represents the free energy of the excitons in the quantum well and the second term proportional to the cavity-laser detuning  $\Delta = \omega_c - \omega_p$ , represents the energy of the cavity mode. The third term is the energy of the mechanical resonator described by the dimensionless position  $q$  and momentum,  $p$  operators which satisfy the commutation relation  $[q, p] = i\hbar$ . The fourth and fifth terms describe the coupling of the cavity mode with the exciton and mechanical resonator, respectively. The last term describes the interaction

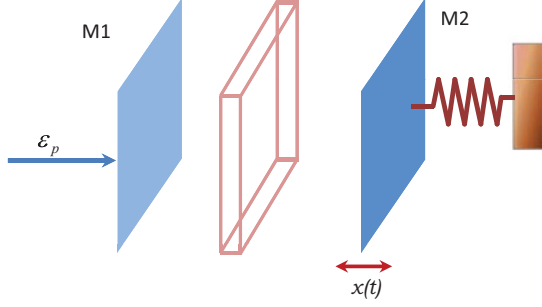


FIG. 1. (Color online) Schematic of optomechanical system coupled to a high-quality cavity containing a quantum well.

of the cavity mode with the pump laser of amplitude  $\varepsilon_p = \sqrt{2\kappa P/\hbar\omega_p}$  with  $2\kappa$  being the cavity decay rate.  $a$  and  $b$  are annihilation operators of the cavity mode and the exciton mode, respectively, and satisfy the commutation relations  $[a, a^\dagger] = 1$  and  $[b, b^\dagger] = 1$ .  $g_m = \beta\sqrt{\hbar/2\omega_m m}$  is the coupling strength between the mechanical resonator and the cavity with  $\beta = \partial\omega_c/\partial x$  and  $m$  resonator effective mass;  $g$  is the coupling constant between the cavity mode and excitons in the quantum well. In order to fully describe the dynamics of the system it is essential to include the fluctuation dissipation processes affecting the optical, mechanical, and exciton modes. Using the Hamiltonian (1) and taking into account dissipation processes, one readily obtains the following quantum Langevin equations:

$$\frac{da}{dt} = -(\kappa + i\Delta)a + ig_m qa - igb + \varepsilon_p + \sqrt{2\kappa}a_{in}, \quad (2)$$

$$\frac{db}{dt} = -(\gamma + i\delta_b)b - ig a + \sqrt{2\gamma}b_{in}, \quad (3)$$

$$\frac{dp}{dt} = -\gamma_m p - \omega_m q + g_m a^\dagger a + \xi(t), \quad (4)$$

$$\frac{dq}{dt} = \omega_m p, \quad (5)$$

where  $2\gamma$  is the spontaneous decay rate of excitons and  $a_{in}$  and  $b_{in}$  are input vacuum noise whose nonzero correlation functions in the frequency domain are given by

$$\langle a_{in}(\omega)a_{in}^\dagger(\omega') \rangle = 2\pi\delta(\omega - \omega'), \quad (6)$$

$$\langle b_{in}(\omega)b_{in}^\dagger(\omega') \rangle = 2\pi\delta(\omega - \omega'). \quad (7)$$

The mechanical mode is affected by a viscous force of damping rate  $\gamma_m$  and by a Brownian stochastic force with zero-mean  $\xi$ . This Brownian force is, in general, a non-Markovian Gaussian noise [10], however, in the limit of a large mechanical quality factor  $Q_m = \omega_m/\gamma_m \gg 1$  the correlation function in the frequency domain can be written to a good approximation as

$$\langle \xi(\omega)\xi(\omega') \rangle \simeq \gamma_m(2n_{th} + 1)\delta(\omega + \omega'), \quad (8)$$

where  $n_{th} = [\exp(\hbar\omega_m/k_B T) - 1]^{-1}$  is the mean number of thermal photons with  $k_B$  being the Boltzmann constant.

### III. OPTICAL BISTABILITY INDUCED BY OPTOMECHANICAL COUPLING

Optical bistability in semiconductor microcavities has been observed experimentally [24]. There are several mechanisms

that would lead to bistable behavior in these systems. One possible mechanism is creating nonlinearity in the system which can be achieved by increasing the density of exciton which results in exciton-exciton scattering. An alternative way to create the bistable behavior is via bleaching of the Rabi splitting [2]. Earlier, Gibbs *et al.* [25] demonstrated room temperature optical bistability of the intracavity photon number in semiconductor microcavities. Here we propose an alternative scheme for realization of optical bistability using the mechanical modes of a vibrating mirror of the cavity in a regime where the earlier proposals fail. In essence it is the nonlinearity due to optomechanical coupling that is responsible for bistability behavior in this scheme.

Solving the expectation values of Eqs. (2)–(5) in the steady state we obtain

$$\langle a \rangle = \frac{\varepsilon_p}{\kappa_0 + i(\Delta_0 - \frac{2g_m^2 I_a}{\omega_m})}, \quad (9)$$

where  $I_a = |\langle a \rangle|^2$  is the mean intracavity photon number in the steady state,  $\kappa_0 = \kappa + \lambda^2\gamma$  and  $\Delta_0 = \Delta - \lambda^2\delta_b$  with  $\lambda^2 = g^2/(\gamma^2 + \delta_b^2)$ . It then follows from (9) that

$$I_a \left[ \kappa_0^2 + \left( \Delta_0 - \frac{2g_m^2 I_a}{\omega_m} \right)^2 \right] = |\varepsilon_p|^2. \quad (10)$$

Since this equation is cubic in  $I_a$  the system may exhibit bistability for a certain parameter range. As can be seen from Eq. (10), the bistability in the intracavity photon number disappears when we set  $g_m = 0$ . To clearly see the regime where the system exhibits bistability behavior we next derive the bistability condition for our scheme. Imposing the condition that  $\partial|\varepsilon_p|^2/\partial I_a = 0$ , we obtain

$$\kappa_0^2 + \Delta_0^2 - \frac{8g_m^2 \Delta_0 I_a}{\omega_m} + \frac{12g_m^4 I_a^2}{\omega_m^2} = 0. \quad (11)$$

Therefore, the system can exhibit bistability when the discriminant of the above quadratic equation is positive, which gives the bistability condition as

$$\frac{g_m^4}{\omega_m^2} (\Delta_0^2 - 3\kappa_0^2) > 0. \quad (12)$$

We immediately see from this equation that the bistability condition fails if  $g_m = 0$  or  $\omega_m \gg g_m$ . Thus the presence of the mechanical modes is imperative for the system to exhibit bistability behavior. Assuming the coupling constant  $g_m$  is nonzero and the frequency  $\omega_m$  is finite, the bistability condition can be written as  $\Delta_0^2 - 3\kappa_0^2 > 0$  or explicitly,

$$\Delta^2 - 3\kappa^2 - 2\lambda^2(\Delta\delta_b + 3\kappa) + \lambda^4(\delta_b^2 - 3\gamma^2) > 0. \quad (13)$$

We first consider a special case in which we remove the quantum well from the cavity, that is, no photon-exciton coupling ( $g = 0$ ). The bistability condition, setting  $\lambda = 0$  in Eq. (13), reduces to

$$\Delta^2 - 3\kappa^2 > 0. \quad (14)$$

This is simply the optical bistability condition for the optomechanical cavity without the quantum well. In Fig. 2(a), the intracavity mean photon number versus the cavity-pump laser detuning  $\Delta$  for pump intensity  $P = 10$  nW is illustrated.

When the pump laser intensity is  $P = 10$  nW the curve is nearly Lorentzian. However, for sufficiently strong input pump laser power, the cubic equation for the mean intracavity photon number Eq. (10) yields three real roots, which is a signature of bistable behavior. The smallest and largest roots are stable while the middle one is unstable. Graphically, as the pump laser power increases the spectra of the mean photon number become asymmetric and gives rise to three possible values [see Fig. 2(a)]. We also see from this figure that for the bistable behavior to occur, large cavity-pump detuning is necessary with the corresponding large-pump laser power. The bistable behavior can also be seen from the mean intracavity photon number versus the pump power curve [see Fig. 2(b)]. Here we have taken the cavity-pump laser detuning to be  $\Delta = \omega_m$ , an appropriate regime for cooling the mechanical resonator close to the quantum ground state [26]. As can be seen from Fig. 2(b), the system exhibits optical bistability for large-pump laser power. The bistability can be obtained by scanning the input pump power in two directions. For example, by gradually increasing the pump power from zero to a sufficiently strong pump power, in our case, for parameters given in Fig. 2(b), about  $\sim 1.85$   $\mu$ W, one finds the lower bistable point. The hysteresis then follows the arrow and jumps to the upper branch. To obtain the other unstable point, one needs to scan the input pump power to lower values, which appears at  $\sim 100$  nW. Note that the position of the bistable points strongly relies on cavity-pump laser detuning and other system parameters.

We next proceed to study the effect of the presence of the quantum well in the cavity on the optomechanical bistability.

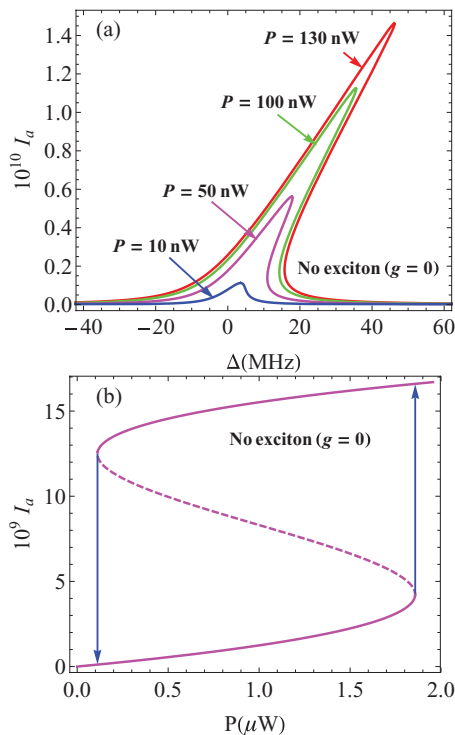


FIG. 2. (Color online) Plots of the mean intracavity photon number versus (a) cavity-pump laser detuning  $\Delta$  (MHz) for various values of the pump-laser power (b) input pump power for cavity-pump laser detuning  $\Delta = \omega_m$ . Other parameters are  $\kappa = 2\pi \times 10^5$  Hz,  $g_m = 250$  Hz,  $\omega_m = 2\pi \times 6.3$  MHz,  $\gamma_m = 40$  Hz, and  $\delta_b = 0$ .

Here we choose experimentally realizable parameters for optomechanical systems [27] with the high quality factor  $Q_m = \omega_m/\gamma_m = 10^6$ . We also assume that the frequency of the mechanical mode  $\omega_m$  is greater than the cavity decay rate  $2\kappa$  so that the system would be in the good cavity limit, a prerequisite for resolved sideband cooling of micromechanical resonators [28].

The effect of the presence of a quantum well is presented in Fig. 3. In Fig. 3(a), we plot the mean intracavity photon number as a function of cavity-pump detuning  $\Delta$  for input pump power  $P = 300$  nW. This figure clearly shows that the system exhibits optical bistability for sufficiently large exciton-pump detuning. The bistable behavior disappears near the exciton-cavity resonance ( $\delta_b \sim 0$ ). It is also interesting to see that the regime for which the bistability occurs strongly relies on the value of the exciton-pump detuning. The larger the detuning, the wider the power range for which the bistability appears. This can be understood by looking at the bistability condition given by Eq. (13). If the term  $\lambda^4(\delta_b^2 - 3\gamma_b^2)$  is less than zero, then the presence of the exciton appears to destroy or diminish the bistable behavior depending on the cavity-exciton coupling strength  $g$  or  $\lambda$ . In order to make this term positive, exciton-pump detuning should satisfy the inequality  $\delta_b^2 > 3\gamma_b^2$ , which is the bistability condition for semiconductor microcavity containing a quantum well [24]. Thus the bistability condition for our scheme can be satisfied if the contribution of the term  $\lambda^4(\delta_b^2 - 3\gamma_b^2)$  is sufficiently large

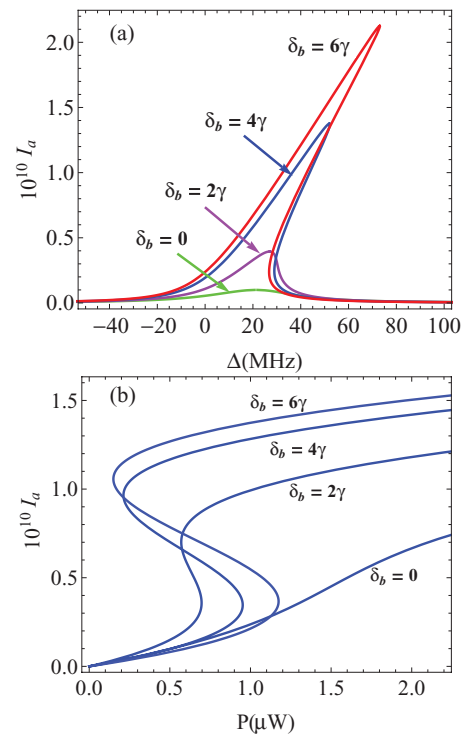


FIG. 3. (Color online) Plots of mean intracavity photon number versus (a) the cavity-pump laser detuning for input power  $P = 300$  nW (b) input pump power for cavity-pump laser detuning  $\Delta = \omega_m$ . Other parameters are  $\gamma = 3.6$  MHz,  $g = 10\gamma$ ,  $\kappa = 2\pi \times 10^5$  Hz,  $g_m = 250$  Hz,  $\omega_m = 2\pi \times 6.3$  MHz,  $\gamma_m = 40$  Hz, and for various values of cavity-exciton detuning  $\delta_b$ . The bistable behavior disappears near the exciton-pump resonance.

positive. Furthermore, the dependence of the mean intracavity photon number on the input pump power is illustrated in Fig. 3(b). This figure reveals that for cavity-pump detuning fixed at  $\Delta = \omega_m$  the intracavity mean photon number exhibits bistability for nonzero exciton-pump detuning  $\delta_b$ . As the detuning  $\delta_b$  increases, the minimum pump power for which the bistability occurs increases. This also confirms our earlier assertion that the exciton-pump detuning has to be large enough to observe the bistable behavior indicating, in addition to the pump power, the pump frequency can be used to control the bistable behavior.

#### IV. INTENSITY AND FLUCTUATION SPECTRA

Here we study the intensity and squeezing spectra of the transmitted field. We first linearize the quantum Langevin equation by writing the operators as the sum of their mean values and the corresponding fluctuation operators, that is,  $a = \langle a \rangle + \delta a$ ,  $b = \langle b \rangle + \delta b$ ,  $p = \langle p \rangle + \delta p$ , and  $q = \langle q \rangle + \delta q$ . In view of this the linearized Langevin equations for the fluctuation operators read

$$\delta \dot{a} = -[\kappa + i(\Delta - g_m \langle q \rangle)] \delta a + iG \delta q - i g \delta b + \sqrt{2\kappa} a_{in}, \quad (15)$$

$$\delta \dot{b} = -(\gamma + i\delta) \delta b - i g \delta a + \sqrt{2\gamma} b_{in}, \quad (16)$$

$$\delta \dot{p} = -\gamma_m \delta p - \omega_m \delta q + G^* \delta a + G \delta a^\dagger + \xi, \quad (17)$$

$$\delta \dot{q} = \omega_m \delta p, \quad (18)$$

where  $\langle q \rangle = g_m I_a / \omega_m$  and  $G = g_m \langle a \rangle$ . Since we are interested in spectra of the transmission field, it is more convenient to work in the frequency domain. To this end, we write Eqs. (15)–(18) in the Fourier space, which can be written in matrix form as

$$\mathbf{M}(\omega) \mathbf{X}(\omega) = \mathbf{N}(\omega), \quad (19)$$

where  $\mathbf{X}(\omega) = (\delta a, \delta a^\dagger, \delta b, \delta b^\dagger, \delta p, \delta q)^T$ ,  $\mathbf{N}(\omega) = (\sqrt{2\kappa} a_{in}, \sqrt{2\kappa} a_{in}^\dagger, \sqrt{2\gamma} b_{in}, \sqrt{2\gamma} b_{in}^\dagger, \xi, 0)^T$ , and

$$\mathbf{M} = \begin{pmatrix} \eta_+ & 0 & i g & 0 & 0 & -i G \\ 0 & \eta_- & 0 & i g & 0 & i G^* \\ i g & 0 & \nu_+ & 0 & 0 & 0 \\ 0 & -i g & 0 & \nu_- & 0 & 0 \\ -G^* & -G & 0 & 0 & i\omega + \gamma_m & \omega_m \\ 0 & 0 & 0 & 0 & -\omega_m & i\omega \end{pmatrix}, \quad (20)$$

where

$$\eta_\pm = \kappa + i(\omega \pm \Delta_{\text{eff}}), \quad (21)$$

$$\nu_\pm = \gamma + i(\omega \pm \delta_b), \quad (22)$$

and the effective detuning is given by

$$\Delta_{\text{eff}} = \Delta - g_m^2 I_a / \omega_m. \quad (23)$$

Solving the matrix equation straightforwardly we obtain the solution for the cavity field fluctuation operator  $\delta a$  to be

$$\delta a(\omega) = \zeta_1 a_{in} + \zeta_2 a_{in}^\dagger + \zeta_3 b_{in} + \zeta_4 b_{in}^\dagger + \zeta_5 \xi, \quad (24)$$

where the coefficients are given by

$$\zeta_1 = \frac{\sqrt{2\kappa} \nu_+}{d} \{ (g^2 + \nu_- \eta_-) [\omega_m^2 + \omega(i\gamma_m - \omega)] + i|G|^2 \omega_m \nu_- \}, \quad (25)$$

$$\zeta_2 = i \frac{\sqrt{2\kappa}}{d} G^2 \nu_+ \nu_- \omega_m, \quad (26)$$

$$\zeta_3 = -i \frac{\sqrt{2\gamma} g}{d} \{ (g^2 + \nu_- \eta_-) [\omega_m^2 + \omega(i\gamma_m + \omega)] + i|G|^2 \omega_m \nu_- \}, \quad (27)$$

$$\zeta_4 = -\frac{\sqrt{2\gamma} g}{d} G^2 \nu_+ \omega_m, \quad (28)$$

$$\zeta_5 = \frac{iG \nu_+ \omega_m}{d} [g^2 + \eta_- \nu_-], \quad (29)$$

$$d = (g^2 + \nu_+ \eta_+) (g^2 + \nu_- \eta_-) [\omega(i\gamma_m - \omega) + \omega_m^2] - i|G|^2 \omega_m [g^2 (\nu_+ - \nu_-) - \nu_+ \nu_- (\eta_+ - \eta_-)]. \quad (30)$$

The solution (24) together with its Hermitian conjugate  $\delta a^\dagger(\omega)$  suffice to study the intensity and squeezing spectra of the transmitted field.

##### A. Intensity spectrum of transmitted field

The intensity spectrum of the transmitted field is given by the Fourier transform of the two time correlation functions,  $\langle \delta a_{\text{out}}^\dagger(t + \tau) \delta a_{\text{out}}(t) \rangle$ :

$$S(\omega) = \int_{-\infty}^{\infty} \langle \delta a_{\text{out}}^\dagger(t + \tau) \delta a_{\text{out}}(t) \rangle e^{-i(\omega - \omega_0)\tau} d\tau. \quad (31)$$

Using the standard input-output relation  $\hat{a}_{\text{out}} = \sqrt{2\kappa} \hat{a} - \hat{a}_{\text{in}}$  [30], the power spectrum can be written as

$$S(\omega) = 2\kappa \int_{-\infty}^{\infty} \langle \delta a^\dagger(t + \tau) \delta a(t) \rangle e^{-i(\omega - \omega_0)\tau} d\tau = 2\kappa C_{a^\dagger a}(\omega), \quad (32)$$

where  $2\pi C_{a^\dagger a}(\omega) \delta(\omega + \omega') = \langle \delta a^\dagger(\omega) \delta a(\omega') \rangle$ . Note that the expression for  $\delta a^\dagger(\omega)$  can be obtained from the expression for  $\delta a$ , by invoking the property of the Fourier transform  $\int_{-\infty}^{\infty} \xi_i^*(\tau) e^{-i\omega\tau} d\tau = \xi_i^*(-\omega)$ :

$$\delta a^\dagger(\omega) = \zeta_1^*(-\omega) a_{in}^\dagger + \zeta_2^*(-\omega) a_{in} + \zeta_3^*(-\omega) b_{in}^\dagger + \zeta_4^*(-\omega) b_{in} + \zeta_5^*(-\omega) \xi. \quad (33)$$

Making use of the correlation properties for noise forces and Eqs. (24) and (33), the intensity spectrum can be put in the form,

$$S(\omega) = 2\kappa [|\zeta_2(-\omega)|^2 + |\zeta_4(-\omega)|^2 + \gamma_m (2n_{\text{th}} + 1) |\zeta_5(-\omega)|^2]. \quad (34)$$

Here we are interested in the spectrum of the transmitted field in the regime where the system is stable or the bistability condition (13) fails. In other words, when the cubic equation for the mean intracavity photon number has one real and two complex roots. For example, as shown in Fig. 3, when the exciton-laser detuning is zero ( $\delta_b = 0$ ), the system is stable (i.e.,  $I_a$  has one real root). In addition, we assume that the exciton-cavity mode coupling is large enough that the system

is in the strong coupling regime,  $g \gg \gamma, \kappa$ . It is well known that, in the strong coupling regime, due to strong exchange of photons between the cavity mode and the excitons, the exciton-cavity coupled system (polariton) emission spectrum consists of two symmetric peaks separated by  $2\sqrt{g^2 + \delta_b^2/4}$  [29]. In our system, in addition to these polariton resonances, there are resonances due to the exchange of energy between the cavity and the mechanical modes or optomechanical resonances.

In order to understand the physics behind the transmitted field spectrum and account for all peaks that would appear in the spectrum, we assume that the photon fluctuation does not affect that of the mechanical fluctuation appreciably. In effect, the evolution of the momentum fluctuation in Eq. (17) can approximately be written as

$$\delta \dot{p} \simeq -\gamma_m \delta p - \omega_m \delta q + \xi. \quad (35)$$

Other equations (15), (16), and (18) remain unchanged. In this approximation, the evolution matrix (20) takes the form,

$$\mathbf{M}_{\text{apx}} \simeq \begin{pmatrix} \eta_+ & 0 & ig & 0 & 0 & -iG \\ 0 & \eta_- & 0 & ig & 0 & iG^* \\ ig & 0 & \nu_+ & 0 & 0 & 0 \\ 0 & -ig & 0 & \nu_- & 0 & 0 \\ 0 & 0 & 0 & 0 & i\omega + \gamma_m & \omega_m \\ 0 & 0 & 0 & 0 & -\omega_m & i\omega \end{pmatrix}. \quad (36)$$

This shows that the mechanical fluctuation is decoupled from the influence of the optical fluctuations while the mechanical fluctuations are still influencing the optical fluctuations.

It is noteworthy to mention here that the width and position of the peaks are determined by imaginary and real parts of the

eigenvalues of the matrix  $M_{\text{apx}}$ . For  $\delta_b = 0$  the eigenvalues of  $M_{\text{apx}}$  turn out to be

$$\lambda_{1,2} = \frac{i}{2}(\kappa + \gamma) + \frac{1}{2}(\Delta_{\text{eff}} \pm \sqrt{4g^2 + [i(\gamma - \kappa) + \Delta_{\text{eff}}]^2}), \quad (37)$$

$$\lambda_{3,4} = \frac{i}{2}(\kappa + \gamma) - \frac{1}{2}(\Delta_{\text{eff}} \pm \sqrt{4g^2 + [i(\kappa - \gamma) + \Delta_{\text{eff}}]^2}), \quad (38)$$

$$\lambda_{5,6} = \frac{i\gamma_m}{2} \pm \frac{1}{2}\sqrt{4\omega_m^2 - \gamma_m^2}. \quad (39)$$

It is obvious to see from equations that the transmitted field spectral would consist of six peaks corresponding to the six different eigenvalues. It is important to mention here that if we consider two independent systems (optomechanical cavity without quantum well and a cavity containing a quantum well without mirror motion), each system is known to show two resonance peaks in their respective strong coupling regimes. However, the coupling of these two subsystems gives rise to six distinct peaks in the transmitted field spectrum. While such a description gives useful insight into the physics behind the number peaks and the type of resonances that would appear in the system, one has to relax the earlier assumption that the optical fluctuation does not appreciably affect that of the mechanical mode fluctuation, in order to obtain the correct spectral properties. To this end, it is important to emphasize that all spectra plotted in this work are without the aforementioned approximation.

We begin by considering the effect of the exciton-photon coupling on the transmitted spectrum. Figure 4(a)

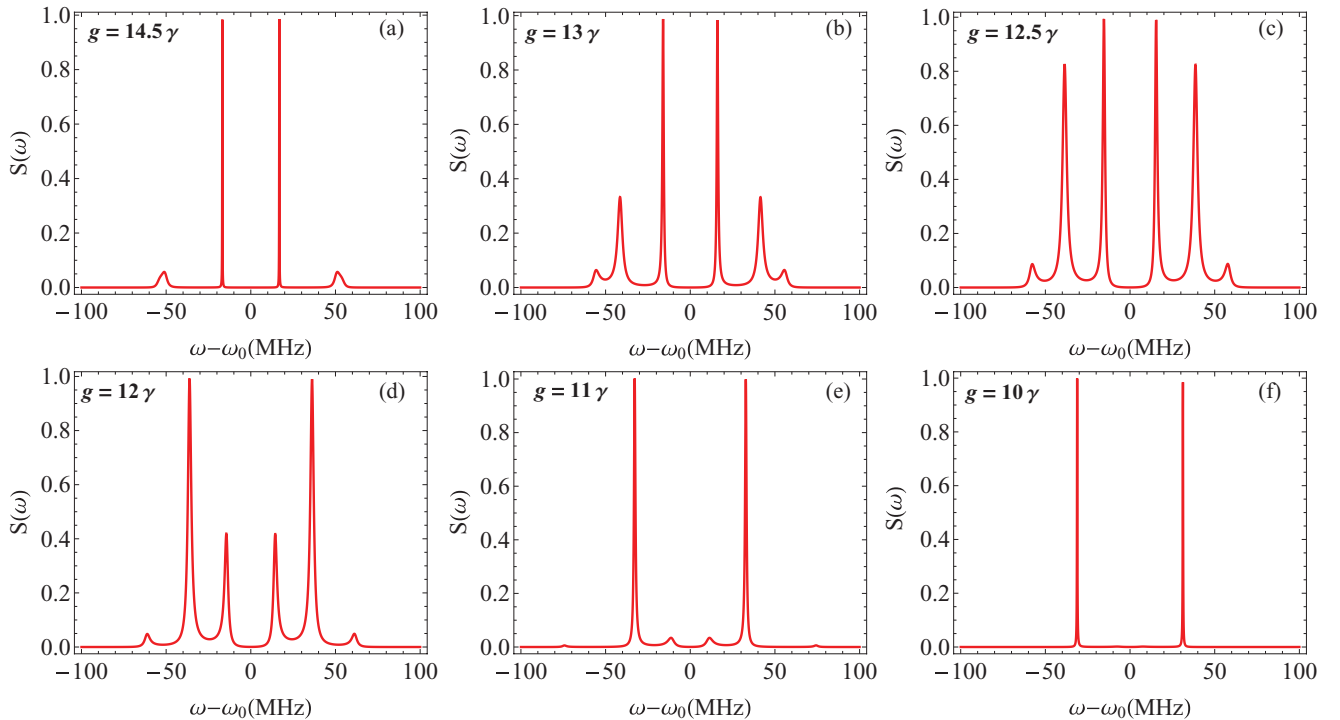


FIG. 4. (Color online) Plots of normalized transmitted field intensity for input pump power  $P = 10$  mW,  $\gamma = 3.6$  MHz,  $\kappa = 2\pi \times 10^5$  Hz,  $g_m = 300$  Hz,  $\gamma_m = 40$  Hz,  $\Delta = \omega_m = 2\pi \times 2.7$  MHz,  $n_{\text{th}} = 175$ ,  $\delta_b = 0$ , and for various values of photon-exciton coupling strength  $g$ : (a)  $g = 14.5\gamma$ , (b)  $g = 13\gamma$ , (c)  $g = 12.5\gamma$ , (d)  $g = 12\gamma$ , (e)  $g = 11\gamma$ , (f)  $g = 10\gamma$ .

illustrates the transmitted field spectrum for  $g = 14.5\gamma$ ,  $\Delta = \omega_m = 2\pi \times 2.7$  MHz,  $\gamma = 3.6$  MHz,  $\gamma_m = 40$  Hz, and  $g_m = 300$  Hz. The two dominant peaks, centered at  $\omega - \omega_0 \sim \pm\omega_m \sim \pm 17$  MHz, represent the optomechanical resonance, while the other two peaks, centered at  $\omega - \omega_0 \sim \pm(\Delta_{\text{eff}} + \sqrt{4g^2 + \Delta_{\text{eff}}^2})/2 \sim \pm 52$  MHz corresponds to the polariton resonances. Since the effective detuning  $\Delta_{\text{eff}}$  is small for large  $g$ , the four peaks corresponding to Eqs. (37) and (38) converge to two peaks for relatively large  $g$ . Thus the optomechanical and the polariton resonances are clearly distinguishable. This can be explained by noting that under strong exciton-photon coupling, there is high photon density that induces strong photon pressure on the resonator which enhances the amplitude of the mechanical mode leading to optomechanical resonance. If one decreases the exciton-photon coupling to  $g = 13\gamma$ ,  $\Delta_{\text{eff}}$  becomes larger and two small side peaks start to split leading to the formation of four hybrid peaks involving cavity, exciton, and mechanical modes as shown in Fig. 4(b). For a slight decrease in the coupling constant  $g$ , the hybrid peaks become very distinct and two of the four peaks centered at  $\omega - \omega_0 \sim \pm(\Delta_{\text{eff}} - \sqrt{4g^2 + \Delta_{\text{eff}}^2})/2 \sim \pm 40$  MHz emerge stronger [see Fig. 4(c)].

It is interesting to note that as the coupling  $g$  decreases further the photon density in the cavity decreases and hence the radiation pressure leading to a decrease in the amplitude of the optomechanical resonance at the expense of enhanced amplitude for the dominant hybrid resonance, as shown in Fig. 4(d). Figure 4(e) shows that for  $g = 11\gamma$  not only the optomechanical resonance but also the amplitude of the two hybrid peaks becomes smaller. This signifies the first stage for disappearance of the pure optomechanical and polariton resonances and emergence of hybrid resonance. Finally, as shown in Fig. 4(f), when the exciton-photon coupling reaches to  $g = 10\gamma$ , the pure optomechanical as well as polariton resonance completely disappear and a strong hybrid resonance emerges. This is one of the main results of this work.

In order to see the effect of pump-laser power on the transmitted field spectrum, we plot in Fig. 5 the transmitted field spectrum for various pump power strength. Figures 5(a)–5(c) represent the transmitted spectrum for pump power  $P = 10$  mW, 15 mW, and 20 mW, respectively. We note from these figures that when the pump power increases, the amplitude of the normalized optomechanical resonance peaks as well as the

small side hybrid peaks start to decrease while the amplitude of the dominant hybrid peaks remain unaffected. In addition, an increase in the pump power gives rise to a shift in the hybrid resonance frequencies—the frequencies of the small hybrid peaks become larger while that of the dominant peaks gets smaller. This can be understood by noting that the splitting between the blue- and red-detuned peaks is proportional to the optomechanical ( $g_m$ ) as well as exciton-photon ( $g$ ) coupling. These couplings are strongly dependent on the pump power or the number of photons in the cavity. The higher the number of photons in the cavity, the stronger these couplings become and hence the larger the separation between the blue- and red-detuned hybrid peaks.

### B. Quadrature squeezing of transmitted field

The analysis of Sec. III has been used effectively to illustrate the bistable behavior in the mean intracavity photon number which is attributed to the nonlinearity due to the optomechanical coupling. In this section, we further continue to explore the consequence of this nonlinearity by considering another nonclassical property. In particular, we analyze the squeezing properties of the transmitted field, which is accessible to experiment and useful for practical applications. The squeezing spectrum of the transmitted field is given by

$$\begin{aligned} S_\theta(\omega) &= \int_{-\infty}^{\infty} \langle \delta X_\theta^{\text{out}}(t + \tau) \delta X_\theta^{\text{out}}(t) \rangle_{\text{ss}} e^{-i\omega\tau} d\tau \\ &= \langle \delta X_\theta^{\text{out}}(\omega) \delta X_\theta^{\text{out}}(\omega) \rangle, \end{aligned} \quad (40)$$

where  $\delta X_\theta^{\text{out}}(\omega) = e^{-i\theta} \delta a_{\text{out}}(\omega) + e^{i\theta} \delta a_{\text{out}}^\dagger(\omega)$  is an experimentally measurable quadrature of the field with  $\theta$  being its externally controllable phase angle.

It is more convenient to work in the frequency domain in part because the coupled differential equations given by Eqs. (15)–(18) would become simple linear equations. Besides, experimentally, fluctuations of the electric field are more convenient to measure in the frequency domain than in the time domain. The squeezing spectrum can then be rewritten as

$$S_\theta(\omega) = 1 + 2C_{a^\dagger a}^{\text{out}} + e^{-2i\theta} C_{aa}^{\text{out}} + e^{2i\theta} C_{a^\dagger a^\dagger}^{\text{out}}, \quad (41)$$

where  $\langle \delta \hat{a}_{\text{out}}(\omega) \delta \hat{a}_{\text{out}}(\omega') \rangle = 2\pi \delta(\omega + \omega') C_{aa}^{\text{out}}(\omega)$  and other terms are defined in a similar way. In experiment the squeezing can be measured by beating the field output from the cavity

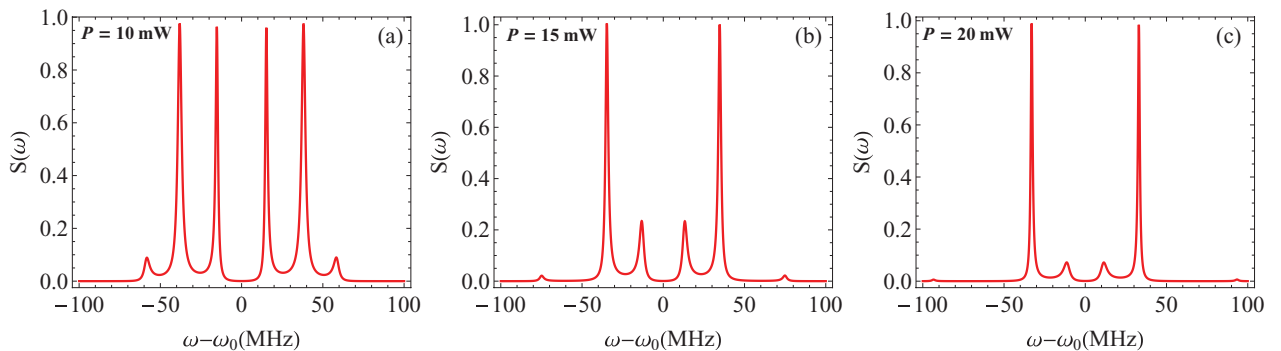


FIG. 5. (Color online) Plots of transmitted field intensity for  $g = 12.4\gamma$  and for various input pump power: (a)  $P = 10$  mW, (b)  $P = 15$  mW, (c)  $P = 20$  mW. Other parameters are the same as in Fig. 4.

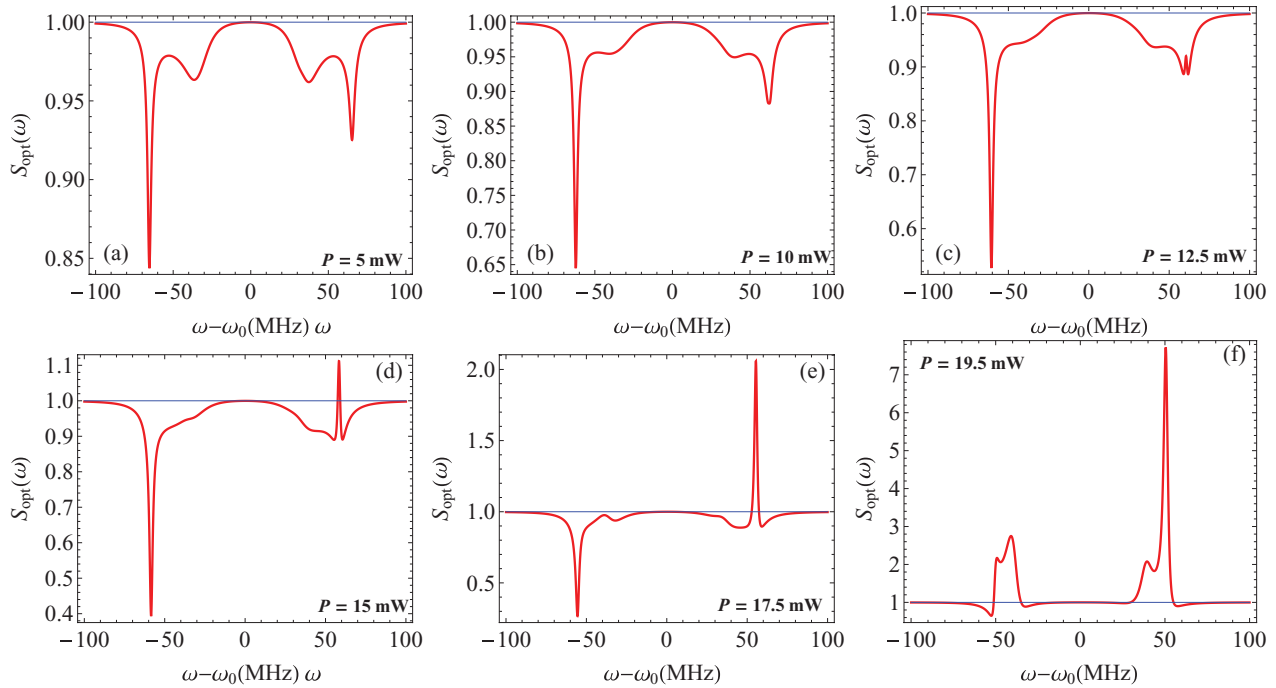


FIG. 6. (Color online) Plots of squeezing spectrum of the transmitted field for  $g = 12.4\gamma$ ,  $\Delta = \omega_m = 2\pi \times 6.3$  MHz, and for various input pump powers: (a)  $P = 5$  mW, (b)  $P = 10$  mW, (c)  $P = 12.5$  mW, (d)  $P = 15$  mW, (d)  $P = 17.5$  mW, and (e)  $P = 19.5$  mW. Other parameters are the same as in Fig. 4.

with a local oscillator field of reference frequency  $\omega_c$  and reference phase angle  $\theta$ . In effect,  $\omega_c$  is the cavity resonance frequency and  $\theta$  is an external parameter which can be used to control the degree of squeezing. Now we optimize the squeezing spectrum with respect to the phase angle  $\theta$ . To this end, we solve for  $\theta$  from  $dS_\theta(\omega)/d\theta = 0$ . This yields

$$e^{2i\theta_{\text{opt}}} = \pm \frac{C_{aa}^{\text{out}}(\omega)}{|C_{aa}^{\text{out}}(\omega)|}. \quad (42)$$

Since we are looking for a solution which minimizes the spectrum function, we choose the minus solution. Thus, the optimized spectrum becomes

$$S_{\text{opt}}(\omega) = 1 + 2C_{a^1a}^{\text{out}}(\omega) - 2|C_{aa}^{\text{out}}(\omega)|. \quad (43)$$

Using the solutions (24) and (33), the optimum squeezing spectrum takes the form,

$$S_{\text{opt}}(\omega) = 1 + 4\kappa \left[ |\zeta_2(-\omega)|^2 + |\zeta_4(-\omega)|^2 + \gamma_m(2n_{\text{th}} + 1)|\zeta_5(-\omega)|^2 - \left| \zeta_1(\omega)\zeta_2(-\omega) + \zeta_3(\omega)\zeta_4(-\omega) - \frac{\zeta_2(-\omega)}{\sqrt{2\kappa}} \right| + \gamma_m(2n_{\text{th}} + 1)\zeta_5(\omega)\zeta_5(-\omega) \right]. \quad (44)$$

The quadrature operators are defined in such a way that perfect squeezing corresponds to  $S_{\text{opt}}(\omega) = 0$ . It is noteworthy to mention here that the squeezing that is manifested in our system is exclusively due to the nonlinearity induced by optomechanical coupling. If we turn off the optomechanical coupling ( $g_m = 0$ ), no squeezing will appear.

We next consider the dependence of the degree of squeezing on the pump laser power. For this purpose, we plot the expression for the squeezing spectrum Eq. (44) for various values of the pump power and for realistic parameters:  $\Delta = \omega_m = 2\pi \times 6.3$  MHz,  $g = 12.4\gamma$ ,  $\gamma = 3.6$  MHz,  $k = 2\pi \times 10^5$  Hz,  $g_m = 300$  Hz,  $\gamma_m = 40$  Hz. As can be seen from the series of plots in Fig. 6, the degree of squeezing in general increases with the pump power. For the pump power  $P = 5$  mW and 10 mW the transmitted field exhibits moderate squeezing for all resonance frequencies, with stronger squeezing at the red-detuned frequency [see Figs. 6(a) and 6(b)]. As the pump power is increased further to  $P = 12.5$  mW, the squeezing at the blue-detuned frequency decreases while that at the red-detuned frequency increases as shown in Fig. 6(c). When the pump power reaches  $P = 15$  mW [Fig. 6(d)], the transmitted field shows even stronger squeezing at the red-detuned frequency. However, the squeezing disappears at the blue-detuned frequency. It is important to mention here that for the given parameters, the optimum squeezing is obtained at the hybrid resonance frequencies despite the fact that optomechanical coupling is responsible for the nonlinearity in the system.

Furthermore, an increase in the degree of squeezing is observed at the red-detuned frequency at the expense of enhanced fluctuations in the blue-detuned frequency for pump power  $P = 17.5$  mW as shown in Fig. 6(e). The amount of squeezing obtained in this case is about 75% below the vacuum level. However, if the pump power is increased further from this point on, the squeezing in the red-detuned frequency starts to decrease and gradually disappears as it is depicted in Fig. 6(f). Therefore, we observe from these series of spectra that for a given set of parameters, there is an optimum laser

pump power that would yield a strong squeezing of the transmitted light. This, in particular, it is advantageous in the context of controlling the degree of squeezing by external parameters, in this case the power of the pump laser.

## V. CONCLUSION

In conclusion, we have investigated the bistable behavior of the intracavity mean photon number and the intensity and squeezing spectra of the transmitted field for an optomechanical resonator containing a single quantum well. It turns out that due to the nonlinearity induced by the optomechanical coupling, the system exhibits optical bistability. This nonclassical property can be controlled by tuning the power or frequency of the pump laser. We have derived the general condition for bistability in the presence of the quantum well. Furthermore, we have shown that the spectrum of the transmitted field consists of six distinct peaks that correspond to optomechanical, polariton, and hybrid resonances. Although, the excitons in the

quantum well are not directly coupled to the optomechanical mode, the widths and the positions of the polariton resonances are modified by the optomechanical fluctuations leading to hybrid resonances. This is due to the fact that both the mechanical and excitonic modes are coupled to a common cavity mode. As a result of the nonlinearity induced by the optomechanical coupling, the transmitted field exhibits strong squeezing at certain hybrid resonance frequencies and system parameters. Beyond the fundamental interest, the present scheme can, in principle, be used as an optical switch with the external pump power or frequency as possible external control parameters.

## ACKNOWLEDGMENTS

E.A.S. is supported by the Herman F. Heep and Minnie Belle Heep Texas A&M University Endowed Fund held and administered by the Texas A&M Foundation.

- 
- [1] C. Fabre, M. Pinard, S. Bourzeix, A. Heidmann, E. Giacobino, and S. Reynaud, *Phys. Rev. A* **49**, 1337 (1994).
  - [2] A. Tredicucci, Y. Chen, V. Pellegrini, M. Borger, and F. Bassani, *Phys. Rev.* **54**, 3493 (1996).
  - [3] A. Dorsel, J. D. McCullen, P. Meystre, E. Vignes, and H. Walther, *Phys. Rev. Lett.* **51**, 1550 (1983).
  - [4] P. Meystre, E. M. Wright, J. D. McCullen, and E. Vignes, *J. Opt. Soc. Am. B* **2**, 1830 (1985).
  - [5] C. Jiang, B. Chen, and K.-D. Zhu, *JOSA B* **29**, 220 (2012).
  - [6] V. B. Braginsky, *Measurement of Weak Forces in Physics Experiments* (University of Chicago Press, Chicago, 1977).
  - [7] D. Vitali, S. Gigan, A. Ferreira, H. R. Bohm, P. Tombesi, A. Guerreiro, V. Vedral, A. Zeilinger, and M. Aspelmeyer, *Phys. Rev. Lett.* **98**, 030405 (2007).
  - [8] D. Vitali, P. Tombesi, M. J. Woolley, A. C. Doherty, and G. J. Milburn, *Phys. Rev. A* **76**, 042336 (2007).
  - [9] C. Genes, A. Mari, P. Tombesi, and D. Vitali, *Phys. Rev. A* **78**, 032316 (2008).
  - [10] M. Abdi, Sh. Barzanjeh, P. Tombesi, and D. Vitali, *Phys. Rev. A* **84**, 032325 (2011).
  - [11] G. S. Agarwal and Sumei Huang, *Phys. Rev. A* **81**, 041803(R) (2010).
  - [12] S. Weis, R. Riviere, S. Delglise, E. Gavartin, O. Arcizet, A. Schliesser, and T. J. Kippenberg, *Science* **330**, 1520 (2010).
  - [13] C. Jiang, J.-J. Li, W. He, and K.-D. Zhu, *Euro. Phys. Lett.* **91**, 58002 (2010).
  - [14] A. H. Safavi-Naeini, T. P. Mayer Alegre, J. Chan, M. Eichenfield, M. Winger, Q. Lin, J. T. Hill, D. E. Chang, and O. Painter, *Nature (London)* **472**, 69 (2011).
  - [15] O. Arcizet, P.-F. Cohadaon, T. Briant, M. Pinard and A. Haidmann, *Nature (London)* **444**, 71 (2006).
  - [16] S. Gigan *et al.*, *Nature (London)* **444**, 67 (2006).
  - [17] F. Marquardt, J. P. Chen, A. A. Clerk, and S. M. Girvin, *Phys. Rev. Lett.* **99**, 093902 (2007).
  - [18] L. Tian and H. Wang, *Phys. Rev. A* **82**, 053806 (2010).
  - [19] A. Abramovici *et al.*, *Science* **256**, 325 (1992).
  - [20] G. Amalino-Camelia, *Nature (London)* **398**, 216 (1999).
  - [21] D. Rugar, R. Budakin, H. J. Mamin, and B. Chui, *Nature (London)* **430**, 329 (2004).
  - [22] D. E. Chang, A. H. Safavi-Naeini, M. Hafezi, and O. Painter, *New J. Phys.* **13**, 023003 (2011).
  - [23] S. Globlacher, K. Hammerer, M. R. Vanner, and M. Aspelmeyer, *Nature (London)* **460**, 724 (2009).
  - [24] A. Baas, J. Ph. Karr, H. Eleuch, and E. Giacobino, *Phys. Rev.* **69**, 023809 (2004).
  - [25] H. M. Gibbs *et al.*, *Appl. Phys. Lett.* **41**, 221 (1982).
  - [26] A. Schliesser, R. Riviere, G. Anetsberger, O. Arcizet, and T. J. Kippenberg, *Nat. Phys.* **4**, 415 (2008).
  - [27] T. Rocheleau, T. Ndukum, C. Macklin, J. B. Hertzberg, A. A. Clerk, and K. C. Schwab, *Nature (London)* **463**, 72 (2010).
  - [28] J. D. Teufel, T. Donner, Dale Li, J. H. Harlow, M. S. Allman, K. Cicak, A. J. Sirois, J. D. Whittaker, K. W. Lehnert, and R. W. Simmonds, *Nature (London)* **475**, 359 (2011).
  - [29] E. A. Sete, S. Das, and H. Eleuch, *Phys. Rev. A* **83**, 023822 (2011); H. Eleuch, *Eur. Phys. J. D.* **49**, 391 (2008).
  - [30] D. F. Walls and G. J. Milburn, *Quantum Optics* (Springer-Verlag, Berlin, 1994).